EJN fens European Journal of Neuroscience

European Journal of Neuroscience, Vol. 29, pp. 1560–1567, 2009 doi:10.1111/j.1460-9568.2009.06707.x

MOLECULAR AND DEVELOPMENTAL NEUROSCIENCE

Morphological regionalization using fetal magnetic resonance images of normal developing brains

Hui-Hsin Hu,[1,4] Wan-Yuo Guo,[2,3] Hui-Yun Chen,[1,4] Po-Shan Wang,[6,7,8] Chih-I Hung,[1,4] Jen-Chuen Hsieh[4,5] and Yu-Te Wu[1,4,5]

[1]Department of Biomedical Imaging and of Radiological Sciences, National Yang-Ming University, Taipei, Taiwan, China
[2]Department of Radiology, Taipei Veterans General Hospital, Taipei, Taiwan, China
[3]Faculty of Medicine, School of Medicine, National Yang-Ming University, Taipei, Taiwan, China
[4]Integrated Brain Research Laboratory, Department of Medical Research and Education, Taipei Veterans General Hospital, Taipei, Taiwan, China
[5]Institute of Brain Science, National Yang-Ming University, Taipei, Taiwan, China
[6]The Neurological Institute, Taipei Veterans General Hospital, Taiwan, China
[7]Department of Neurology, School of Medicine, National Yang-Ming University Taipei, Taiwan, China
[8]The Neurological Institute, Taipei Municipal Gan-Dau Hospital, Taiwan, China

Keywords: cerebral volume, curvature, growth rate, gyrification index

Abstract

Regional differences in human brain development during infancy have been studied for many years, but little is known about how regionalization of the brain proceeds during intrauterine life. We investigated the regionalization of cerebral volume and cortical convolutions based on the volumetric magnetic resonance images (MRIs) of 43 fetuses, ranging from 21 to 37 weeks of gestation. Two plausible parcellations of MRI are proposed, and curvature index together with gyrification index are used to quantify the regional cortical convolutions. Our results elucidate that the cortical foldings among different brain regions develop at comparable rates, suggesting a similar uniformity of changes in size of the cortical sheet in these regions over time. On the contrary, the growth of the cerebral volume presents regional difference, with the frontal and parieto-temporal regions growing significantly faster than other regions due to the contribution from expansion of basal ganglia. This quantitative regional information suggests that cerebral volume is not a relevant parameter to measure in relation to gyrification, and that the size of the cortical sheet is more likely to be directly related to cortical folding. The availability of quantitative regional information on normal fetal brains *in utero* will allow clinical application of this information when probing neurodevelopmental disorders in the future.

Introduction

The different growth rates of various brain areas have been suggested to be highly associated with the maturation of brain functions among humans. For example, among pre-term human babies, a regional reduction in brain volume is accompanied by a poorer cognitive outcome (Peterson *et al.*, 2000). Recent neuroimaging studies have reported that normal neonates exhibit faster volumetric development in the occipital and parietal regions than in the prefrontal region, which may relate to more rapid maturation of the visual and motor systems than prefrontal executive functions after birth (Gilmore *et al.*, 2007); such regional information will provide important insights into the development of the human brain.

Abnormal growth in cerebral volume and cortical folding has been described as part of brain pathology. The presence of accelerated brain growth associated with autism has been found to lead to an abnormal enlargement of the cerebral volume (Aylward *et al.*, 2002). Brains with schizophrenia show an abnormal pattern of cortical convolutions (White *et al.*, 2003; Bonnici *et al.*, 2007; Harris *et al.*, 2007; Stanfield *et al.*, 2008). Furthermore, abnormal volumetric development has been linked to fetal brain pathologies, such as Walker–Warburg syndrome and ventriculomegaly (Grossman *et al.*, 2006). During intrauterine life, gyrification formation following an abnormal spatiotemporal schedule would seem to accompany growth retardation (Encha-Razavi & Sonigo, 2003). Thus, psychiatric and neurodevelopmental disorders may be reflected in abnormal growth of cerebral volume and cortical convolutions. Accordingly, a better understanding of regional specificity during the increase in cerebral volume and cortical folding during normal fetal brain development is potentially important.

In this study, we investigated regional specificity and the effect of age on the developing brain during intrauterine life based on two appropriate parcellations. Although regional specificity during the development of brain after birth has been widely studied, little is known about how the regionalization of brain proceeds during intrauterine life, which is the most essential period for neuronal

Correspondence: Prof. Y.-T. Wu, as above.
E-mail: ytwu@ym.edu.tw

Received 4 September 2008, revised 5 February 2009, accepted 12 February 2009

migration and cortico-cortical connection. The greatest difficulty when carrying out regional analysis of brains *in utero* is to parcellate brains appropriately because of the limitations of the imaging techniques. The low spatial resolution and an insufficient signal-to-noise ratio (SNR) from the magnetic resonance images (MRI) are due to the small brain volumes. In this study, we propose two plausible approaches by which parcellation of the MRI volumes of fetal brains can be carried out; it is based on neuro-anatomical landmarks and focuses on anterior–posterior development. Additionally, we investigated the effect of fetal age on the regionalization of the brain by dividing all fetuses into two groups, namely those before the third trimester and those after the third trimester. This is based on a previous *in vitro* study, which indicated that most of the gyri and a growth spurt in brain weight appears during the 26th–28th weeks (Chi *et al.*, 1977); thus, based on this, it would seem that the third trimester is a pivotal period of expansion during brain development.

Materials and methods

Subjects

Fetal cranial MRIs that had been collected between 2004 and 2007 were selected from the database of the Department of Radiology, Taipei Veterans General Hospital. The Internal Ethical Committee of Taipei Veterans General Hospital approved the study, which followed the Declaration of Helsinki guidelines and informed consent had been obtained from the mother. We recruited fetuses that had been examined for non-CNS abnormalities but had undergone an additional MRI examination of the brain and/or had shown suspicious ventricular dilatation on ultrasound, but were regarded as normal fetuses by later MRI. All scans were reviewed by a neuroradiological medical practitioner (W.Y. Guo). The study included 43 fetuses aged from 21 to 37 weeks of gestation (21–22 weeks: five fetuses; 23–24 weeks: nine fetuses; 25–26 weeks: four fetuses; 27–28 weeks: eight fetuses; 29–30 weeks: nine fetuses; 31–32 weeks: three fetuses; 33 weeks: three fetuses; 35–37 weeks: two fetuses). The gestational age was evaluated using the date of MRI scan as well as the expected date of delivery as predicted by prenatal ultrasound scanning. Fetal gender was obtained from either the prenatal ultrasound or by genetic examination. Among the fetuses, 19 were male, 17 were female and seven were of unknown gender (Table 1).

Image acquisition

The scanning sequence was spin echo-based half-Fourier acquisition single-shot turbo spin-echo (SSFSE by GE or HASTE by Siemens) using body phase-arrayed coils, which was the preferred pulse sequence among the various ultrafast imaging techniques (Guo & Wong, 2003; Grossman *et al.*, 2006); the system used was a 1.5-Tesla MR scanner (GE or Siemens). The echo time is 95 ms; repetition time is 11.9 ms. The overall scanning time including maternal positioning was usually kept to about 20 min. Two matrix sizes, 256 × 256 or 512 × 512, were obtained with two FOVs (field of view), 280 × 280 or 400 × 400 mm^2, respectively. Image resolutions were 1.09 × 1.09 mm^2 or 0.78 × 0.78 mm^2. Slices thickness was 4 or 5 mm.

We noted that the slice thickness was much larger than that from preterm or term neonates, which are about 1–1.5 mm (Nishida *et al.*, 2006; Gilmore *et al.*, 2007). Nevertheless, fast MRI scanning *in utero* is necessary in order to reduce the possibility of movement artifacts while scanning without sedation; accordingly, the larger slice thicknesses were able to preserve sufficient SNR for the small image volumes using 1.5T fast MRI scanning.

Table 1. Subject demographics

	All (n = 43)	Male (n = 19)	Female (n = 17)	P-value*
Age (weeks)	27.43 ± 3.93 (22–37)	27.81 ± 3.82 (22–37)	27.56 ± 3.86 (22–35)	0.85

The data are presented as means ± SD (with range in parentheses). The gender of seven of the subjects was not recorded. *Based on a two-tailed Student's t-test.

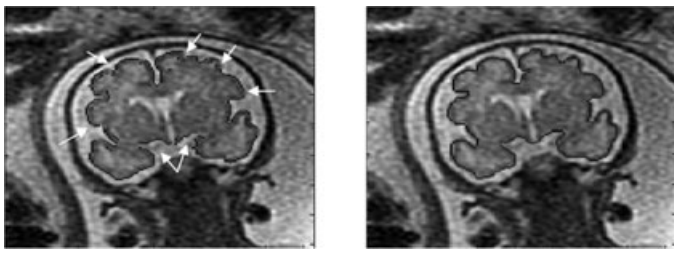

Fig. 1. The results of cerebrum segmentation from a coronal image of a 33-week-old fetus with CNS normality. Left: the black dots (white arrows) is the result of automatic edge detection where parts of the cerebral boundary are discontinuous (white arrows). Right: the final segmentation result after manual intervention (black contour).

Semi-automatic cerebrum extraction

The contour of the cerebrum in the MRI was extracted semi-automatically. The procedure of cerebrum extraction was divided into the following three phases. First, histogram equalization (Gonzales & Woods, 2001) was employed to provide a better contrast for brain delineation. Second, the contour of the fetal cerebral region was automatically detected on each image by Canny edge detection (Canny, 1986), where parts of the cerebral boundary are likely to be discontinuous (the left panel in Fig. 1). Finally, manual assistance was introduced to close the contours in order to complete the segmentation (the right panel in Fig. 1).

A graphical user interface (GUI) was implemented using MATLAB code (MathWorks, Natick, MA, USA) to facilitate the semi-automatic segmentation of cerebral boundary. A GUI was implemented using MATLAB code (MathWorks) to facilitate the semi-automatic segmentation of cerebral boundary. Besides, all algorithms we used for extracting cerebrum were built-in functions in MATLAB. The widely-used Canny edge detection provided additional information related to the contour of cerebrum, which helped us to reduce possible inter-rater or intra-rater errors. In addition, it had the advantage of thinning the gradient edge maps down to the edge with 1 pixel in width.

Parcellation of fetal brain

Coronal image volumes were applied because: (i) they derive more information than sagittal and axial image volumes due to a longer antero-posterior diameter than the superior–inferior and left–right ones; and (ii) they minimize the mingled subregions of the brains. As a result of this approach, we focused on the antero-posterior development of fetal brains in this study.

We propose a new approach to the parcellation of fetal brains based on the premises of two previous studies. The first study by Gilmore *et al.* involved the division of the neonatal brains into four subregions (Fig. 1 in Gilmore *et al.*, 2007) and this was done by transforming the

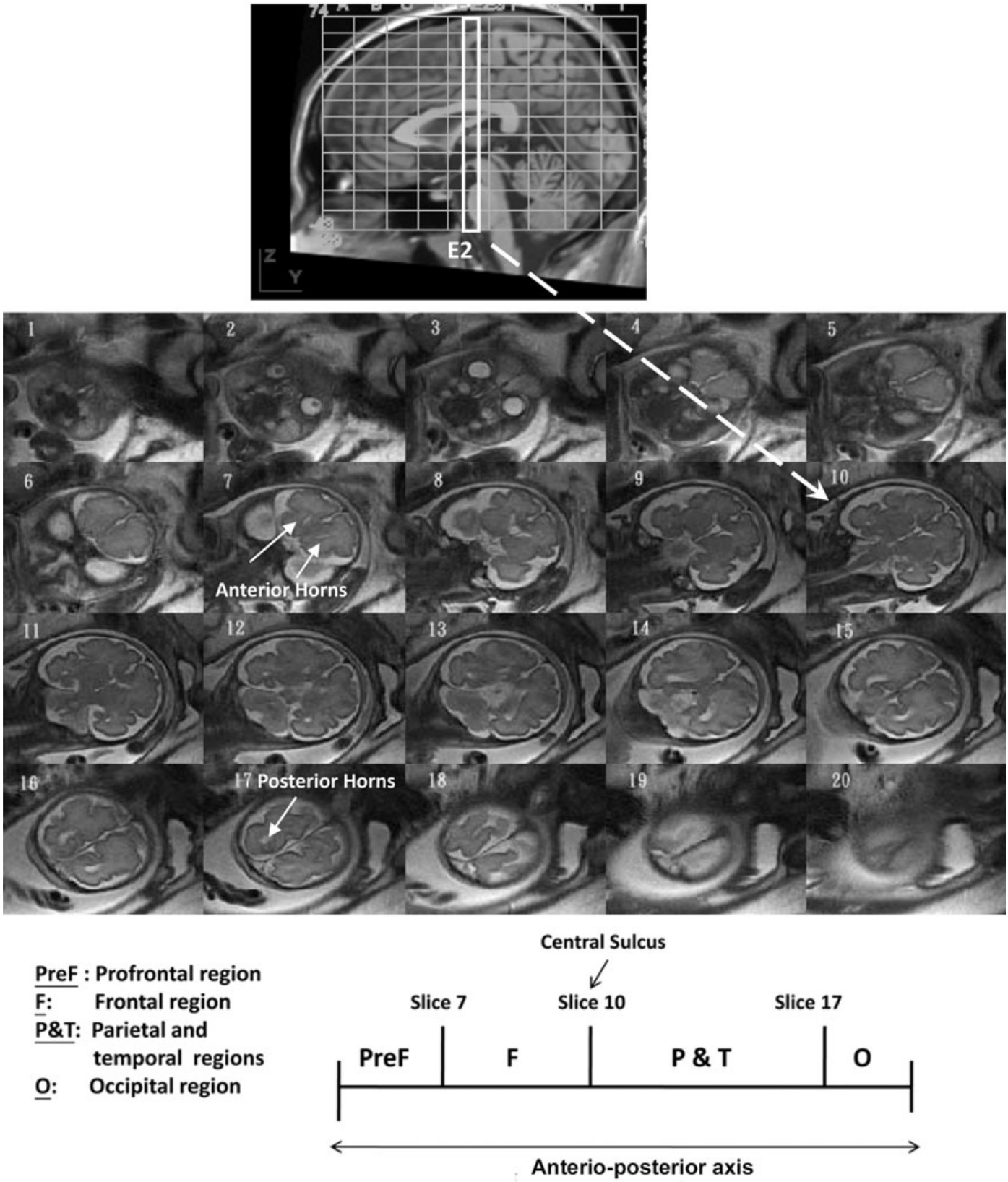

FIG. 2. The antero-posterior parcellations on a 30-week-old fetal brain based on the ventricular system and Talairach grid. This dissects the brain into four subregions, namely, prefrontal (PreF), frontal (F), parieto-temporal (P&T) and occipital (O) regions. Top: the mid-sagittal plane of an adult brain superimposed with the Talairach grids (courtesy of http://www.neurovia.umn.edu/webservice/tal_atlas.html). The E2 block on the Talairach grid comprises the main area of central sulcus. Middle: a series of coronal images of a 30-week-old fetal brain along the antero-posterior axis (slices 1–20). The dashed arrow indicates the corresponding location of central sulcus from adult brain to fetal brain. Bottom: the abbreviations of each subregion (left) and a sketch of parcellations (right) are shown.

neonatal brains into the Talairach atlas. The four brain areas were: (i) the prefrontal region from the most anterior point of the cortex to the lateral ventricles; (ii) the frontal region from the anterior point of the lateral ventricles to the central sulcus; (iii) the parietal region from the central sulcus to the posterior point of the lateral ventricles; and (iv) the occipital region from the posterior point of the lateral ventricles to the occipital pole. The second study by Grossman *et al.*, (2006) involved the ventricular system and reported that this system developed before 22 weeks of gestation and then maintained a steady size during gestation. Motivated by these two studies, we parcellated the fetal brain using an approach similar to that of Gilmore *et al.* (2007); it was based on the spatial position of ventricular system and the Talairach grid using the following three pivotal coronal images.

1. The most anterior slice with lateral horns.
2. The most anterior slice including the third ventricle, the lateral ventricles and brain stem. This slice should encompass the central sulcus based on the position of the central sulcus of adult brain on the Talairach grid. (see the top panel of Fig. 2).
3. The most posterior slice with the lateral horns.

These three slices (slices 7, 10 and 17 in Fig. 2, respectively) dissected the fetal cortex into four subregions, namely, the prefrontal, frontal, parieto-temporal and occipital regions, which are denoted by the PreF, F, P&T and O, respectively (see the bottom panel of Fig. 2).

Morphological indices for the assessment of brain development

Cerebral volume

We obtained the 'cerebral voxels' on each MRI, that is, all voxels inside the red contour in Fig. 1 (right panel). Each fetal cerebral volume was calculated by summing the number of cerebral voxels on the MRI; these were then multiplied by voxel size, which depended on the image resolution and slice thickness.

Gyrification index (GI) and curvature index (CI)

Morphological differences are an alternative way of assessing brain development in addition to cerebral volume. To date, however, there is no gold standard for quantifying shape-related differences within the cerebral cortex. In this study, we employed two popular indices, which have successfully been used to probe the 'local' cortical evolution of adult brain (Zilles *et al.*, 1988; Thompson *et al.*, 1996; Magnotta *et al.*, 1999; Luders *et al.*, 2006), and we anticipated that consistent results would be obtained for validating the growth pattern.

The first index is the GI, which is defined by the ratio of the length of complete cerebral cortex contour to that of outer cortical contour (ignoring the deep sulci; Zilles *et al.*, 1988). To generate the outer contour, the two-dimensional quickhull algorithm was applied to define a convex hull polygon by some points on the inner contour (Batchelor *et al.*, 2002). The second index is intensity-based CI (Thirion & Gourdon, 1993), which is a mathematical quantity that describes the complexity of a curvy graph, and has been applied on the quantification of cortical convolution (Batchelor *et al.*, 2002; Luders *et al.*, 2006). Let the curvature value at a pixel location (x, y) be denoted by $k(x, y)$, and the partial derivatives $\partial f(x,y)/\partial x$ be denoted by f_x, $\partial f(x,y)/\partial y$ by f_y, $\partial^2 f(x,y)/\partial x^2$ by f_{xx}, $\partial^2 f(x,y)/\partial y^2$ by f_{yy} and $\partial^2 f(x,y)/\partial x \partial y$ by $f_{xy}$for simplicity. The curvature value of each pixel on MRI was given by Thirion & Gourdon (1993)

$$k(x,y) = \frac{2f_x f_y f_{xy} - f_x^2 f_{yy} - f_y^2 f_{xx}}{(f_x^2 + f_y^2)^{3/2}}$$

In order to reduce the effect caused by different pixel sizes and inconsistent intensities between images, pixel of each image was rescaled to be the same size followed by binarizing the image intensities, i.e. the gray-scale values of brain were identical among different images. This preprocessing facilitated the calculation of the GI and the CI for each image.

Statistical analyses

Pearson correlation coefficient (R) was calculated to evaluate the chronological relationship between the morphological indices and gestational age. Statistics were calculated using the Matlab Statistical Toolbox (MathWorks), and the level of significance was set to be $P < 0.05$.

Analysis of covariance (ANCOVA) was used to examine the age effect on the whole brain and on the four subregions, as the morphological indices ought to correlate with the gestational age. The age in the ANCOVA was a grouping factor, which divided the cases into two groups, one before and the other after the third trimester watershed. Using ANCOVA, we were able to model measurements as a linear function of gestational age such that the coefficients of regression lines may vary group to group. A multiple comparison procedure was adopted to determine where the differences that appeared by ANCOVA reached significance.

Results

The image quality was optimally tuned to clearly elucidate the chronological features of the sulci and gyri (Fig. 3). The right column in Fig. 4 pictorially shows that the calculation of GI is determined by the ratio of the perimeter of the white areas to that of the gray areas. The middle column of Fig. 4 shows the CI values at 24, 28 and

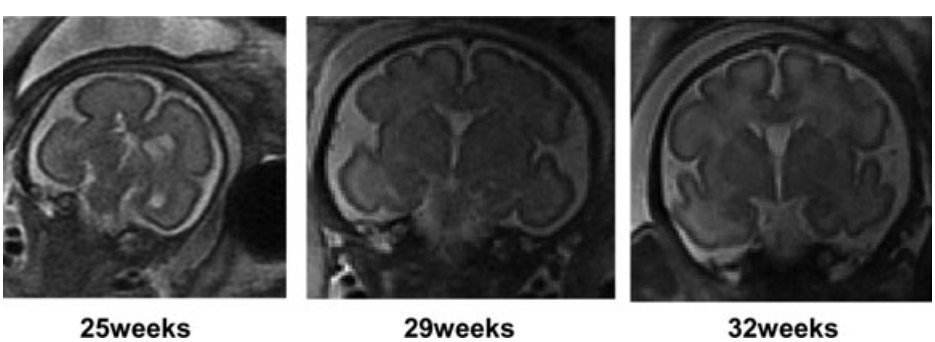

FIG. 3. The chronological features that appear using coronal views. It can be clearly seen that the degree of folding increases with gestational ages.

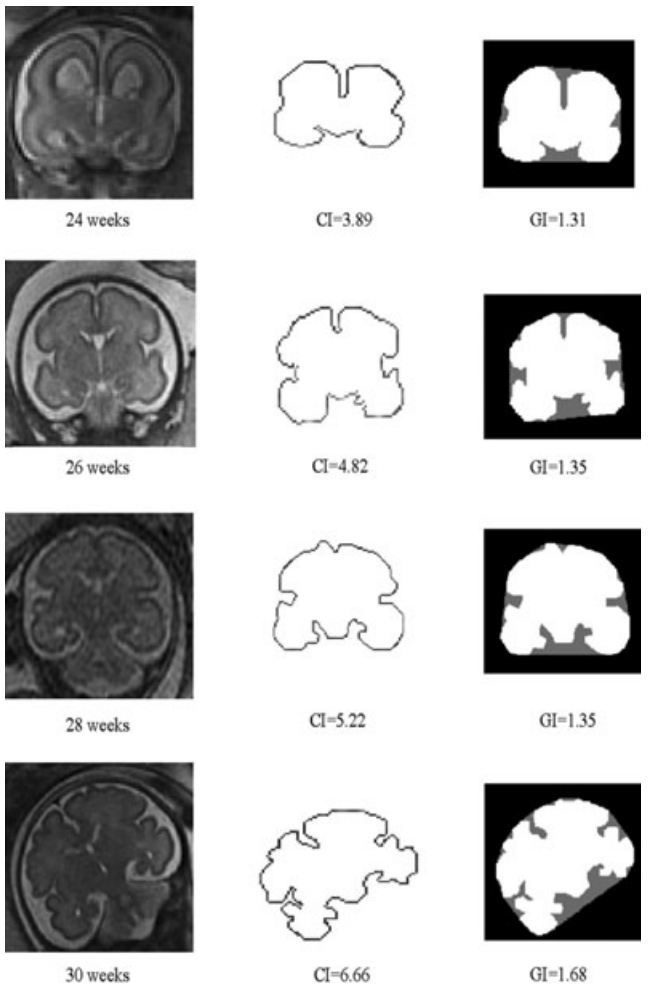

FIG. 4. The corresponding curvature-based indices (CI) and gyrification indices (GI) at different gestational ages during cortical development. Left column: there are four coronal MRI from different fetuses with gestational ages of 24, 26, 28 and 30 weeks. Middle column: estimated CI based on cerebral cortex increases with the complexity of cortical folding. Right column: the GI, which is defined by the ratio of the perimeter of white area to that of gray area, also increases with gestational age.

30 weeks of gestation. We observed that the cortical folding increased with gestational age (Fig. 3) and that the GI/CI values increased with the complexity of cortical contour (Fig. 4).

Significantly age-specific correlation *in utero* was observed in cerebral volume ($R = 0.95$, $P < 0.0001$), averaged CI ($R = 0.88$, $P < 0.0001$) and averaged GI ($R = 0.88$, $P < 0.0001$; Fig. 5). The best-fitting models of cerebral volume, CI and GI vs. gestational age were

$$\text{Cerebral volume} = -4.1948 \times 10^3 - 5.0719 \times 10^3 \times age + 0.342 \times 10^3 \times age^2$$

$$\text{Curvature index} = -2.4335 + 0.1979 \times \text{age}$$

$$\text{Gyrification index} = 0.6276 + 0.0195 \times \text{age}$$

Most of the normative data were within the 95% confidence intervals (dashed curves in Fig. 5). It should be noted that, if the parameters of the GI equation are multiplied by 10, we obtain comparably growing ratios using both methods; that is, the overall gyrification *in utero* increases at a rate of about 0.2 with gestational age.

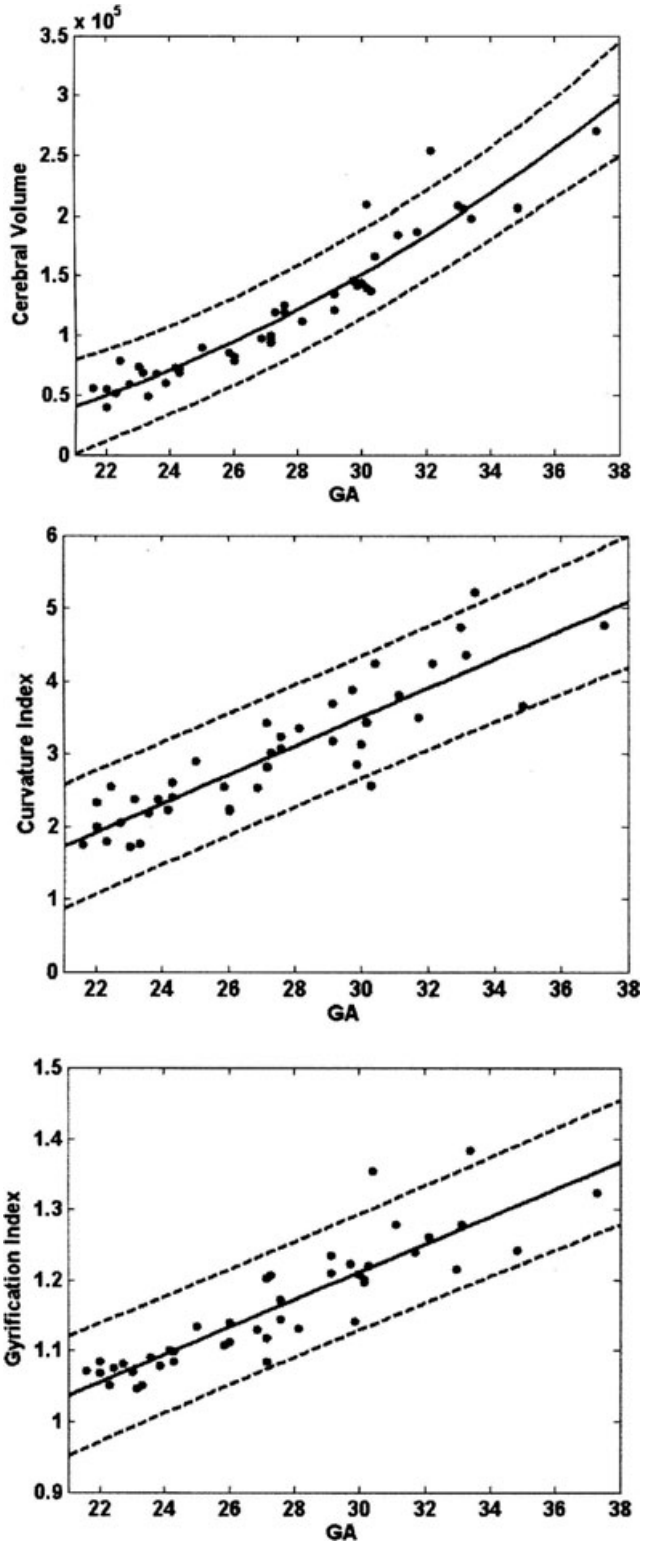

FIG. 5. Age-dependent effects for the different morphological indices across the fetuses. In each plot, the two dashed curves represent the 95% confidence intervals. Top: the quadratic regression is the best fit for the cerebral volume vs. gestational age (GA). A high Pearson's correlation coefficient is observed ($R = 0.95$, $P < 0.0001$). Middle: Curvature index (CI) vs. GA. Linearity between the CI and the GA is found ($R = 0.88$, $P < 0.0001$). Bottom: linear regression between the gyrification index (GI) and GA. The result indicates that GI is a positively age-related index ($R = 0.88$, $P < 0.0001$).

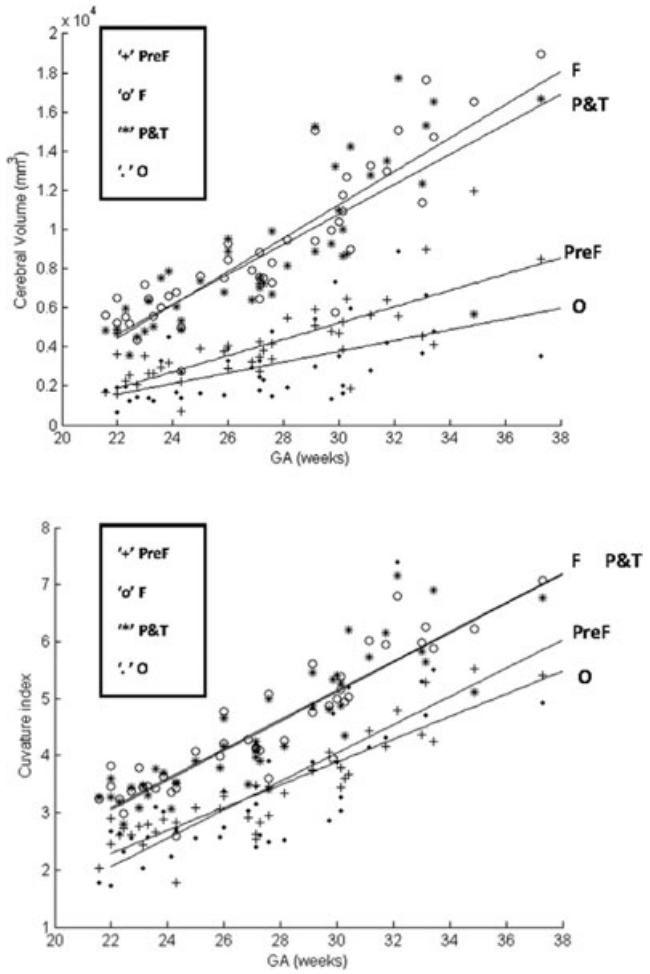

FIG. 6. Regional growth in cerebral volume and cortical folding (CI) obtained from the four-group parcellation of fetal brains into the PreF (prefrontal), F (frontal), P&T (parieto-temporal) and O (occipital) regions. Top: a significantly higher growth rate is observed for the F and P&T regions (ANCOVA: $F_3 = 14.43$, $P < 0.0001$). Bottom: the growth in cortical folding exhibits no significant difference between the distinct subregions of the fetal brain (ANCOVA: $F_3 = 1.68$, $P = 0.1726$).

The regional growth in cerebral volume and gyrification obtained from the four-group parcellation are shown in Fig. 6, in which the slopes of data represent the growth rates and the data values stand for the cerebral volume or the amount of cortical folding (GI/CI). The growth rates of cerebral volume were faster for the F and P&T ($F_3 = 14.42$, $P < 0.0001$) compared with the PreF and O (upper panel in Fig. 6). In contrast to cerebral volume, growth rates of gyrification within the different regions are comparable (CI: $F_3 = 1.68$, $P = 0.1726$; GI: $F_3 = 2.06$, $P = 0.1074$; the lower panels in Fig. 6, the data of GI not shown here). It should be noted, however, that the amount of cortical folding (values of CI/GI) was different between the four subregions at a given age because of the distinct sizes of their cortical surface.

The age effect on the development of the fetal brain was analysed by ANCOVA, and the results are presented in Table 2. The development of the whole cerebral volume accelerated after the third trimester (ANCOVA: $F_1 = 10.97$, $P = 0.002$), especially in the frontal region (ANCOVA: $F_1 = 6.34$, $P = 0.016$). The development of cortical convolutions for whole brain maintained a stable growing rate even after the third trimester ($F_1 = 2.62$, $P = 0.1137$), except for accelerated growth in the prefrontal area (CI: $F_1 = 9.07$, $P = 0.0047$; GI: $F_1 = 11.2$, $P = 0.0047$; Table 2).

TABLE 2. Statistical analyses of age effect by ANCOVA*

Cortical regions	Cerebral volume		CI		GI	
	F-value	*P*-value	*F*-value	*P*-value	*F*-value	*P*-value
Whole brain	10.97	0.002†	2.62	0.1137	1.16	0.6885
PreF	2.34	0.1345	9.07	0.0047†	11.2	0.0047†
F	6.34	0.016†	2.97	0.0925	0.01	0.0927
P&T	0.00	0.9972	0.57	0.4553	1.27	0.2665
O	0.00	0.964	1.36	0.2515	3.39	0.074

*The age effect in ancova is used as a grouping factor by dividing the cases into two groups, those aged less than 28 weeks and those aged more than 28 weeks (d.f. = 1). †Significant age effect. CI, curvature index; F, frontal cortex; GI gyrification index; O, occipital cortex; PreF, prefrontal cortex; P&T, parieto-temporal cortex.

Discussion

The antero-posterior development of the fetal brain manifests itself in regionally specific growth rates for the cerebral volume that appear from the second half of the second trimester to the third trimester. The frontal and parieto-temporal regions enlarge much faster than the other regions during intrauterine life (the upper panel in Fig. 6). This finding is different from the regionalization of cerebral volume during infancy described by a previous study, in which the cerebral volume in occipital region grows faster than the other regions (Gilmore *et al.*, 2007). Although the fetal and infantile brains both reveal regionally specific growth rates, the regionalization process during the fetal stage is different from that during infancy.

The possible reason for the regional difference in cerebral volume, with faster rate in frontal and parieto-occipital regions, can be addressed as follows. Growth in cerebral volume covers the composition of the strata or extracortical structures such as basal ganglia, whereas the change in gyrification reflects aspects of the morphological development of the cortical layer (Caviness, 1975; Armstrong *et al.*, 1991). The basal ganglia develops as a spheroid, ballooning out three-dimensionally, while the pallium, which is the most outer layer that neuroblasts migrate to, follows a planar growth pattern, expanding two-dimensionally (Bradley *et al.*, 1991). Our study exhibits that the increase in size of basal ganglia contributes to the increase in cerebral volume, but not in cortical folding, in the frontal and parieto-temporal regions. (To verify this inference, another three-subdivision parcellation for fetal brains has been proposed. More details and results are described in Fig. 7.) Accordingly, as mentioned above, cerebral volume may not be sufficient to probe changes in cortical convolution at the fetal stages because the measurements of cerebral volume also involve the development of subcortical structure, such as basal ganglia, and the size of cortical sheet is more directly related to cortical folding. As CI/GI did not detect any differences in rate of gyrification in the brain regions (parcellated in both ways used), this may suggest that changes in size of the cortical sheet among brain areas may resemble over time.

Comparable growth rate in cortical folding addressed by the tension-based theory of morphogenesis

Cortical folding may arise from 'tension', as proposed by Van Essen (1997). Such a tension may stem from radial anisotropy where

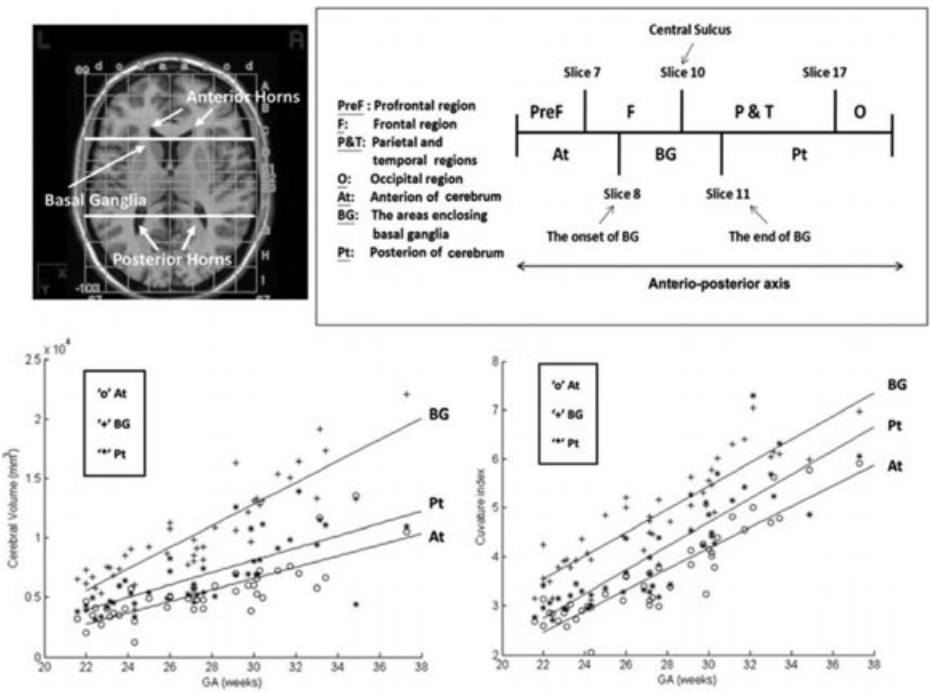

FIG. 7. A three-group parcellation on a 30-week-old fetal brain (the same image data used in Fig. 2) and regional growths of cerebral volume and cortical folding (CI) obtained from this parcellation. The three-group parcellation allows us to extract the area covering most of the basal ganglia and demonstrates that the steeper gradients on the volumes of frontal and temporal/parietal regions would be caused by different growth patterns between basal ganglia and pallium (please see paragraph 2 in Discussion). The brain was segregated into three regions, namely, the basal ganglia (BG), the anterion of cerebrum (At) and the posterion of cerebrum (Pt). To define the onset of basal ganglia, we followed the landmarks of adult brains based on the Talairach atlas. Because the appearances of the basal ganglia followed the anterior horns on the adult brain (top-left panel), the onset of basal ganglia on the fetal brain was identified as the slice next to the one with frontal horns (slice 8 in Fig. 2). The termination was defined as the slice with cerebellum (slice 11 in Fig. 2). It should be noted that the thalamus (slice 12 in Fig. 2) was not taken into account because of its negligible size on the image. Accordingly, we focused only on the development of globus pallidus. Top-left: the axial plane (left) of a mature brain superimposed with the Talairach grids (courtesy of http://www.neurovia.umn.edu/webservice/tal_atlas.html).Top-right: the abbreviations of each subregion (left) and the sketch of two parcellations (right) are exhibited. Bottom-left: statistically regional difference exhibits in growing rates of cerebral volume (ANCOVA: $F_2 = 12.27$, $P < 0.0001$), especially the conspicuous steeper slope in BG. Bottom-right: no regional effect of subregions in cortical folding (CI) is observed (ANCOVA: $F_2 = 0.83$, $P = 0.4393$).

elongation along the radial axis of cellular processes occurs (Van Essen, 1997). Convolutions at specific locations associated with regional boundaries would result from a tangential force component of the tension, which is induced by an oblique axonal direction between adjacent cortical regions after the establishment of the cortico-cortical projection (Van Essen, 1997). In other words, the amount of cortical folding represents the amount of tension along the axons, or the density of the cortico-cortical axons in white matter. Our findings indicate that the amount of cortical convolutions vary from area to area, implying that there are different levels of tension between distinct cortical regions. Besides, the comparable growth rates for cortical folding between the different areas imply a constant tension is sustained during cerebral development, which is in line with the negative feedback mechanism whereby axons adapt their lengths to keep a stable tension (Van Essen, 1997).

The age effect on cerebral volume and gyrification in utero

The age effect mainly involves prefrontal cortical convolutions and frontal cerebral volume during accelerated growth after the third trimester. A previous *in vitro* study has reported a difference for the human cortex from other primates that involves an increase in gyrification of the prefronto-frontal area (Armstrong *et al.*, 1995); accordingly, the age effect on cortical folding may result from the more conspicuous evolution of the prefronto-frontal region among humans. In comparison with the findings of Armstrong *et al.*, our results show an age effect for cortical folding that specifically affects the prefrontal lobe and not the frontal lobe. This inconsistency could be due to Armstrong *et al.*'s equal parcellation of the brain into three parts along the fronto-occipital axis, which results in an inability to separate the prefrontal region from the frontal one. In addition, it is rational to suggest that the development of the prefrontal lobe may be affected by abnormal changes that arise during the third trimester as this period is critical for the development of the cortical convolutions in the prefrontal area. This postulation is congruent with a previous study showing that preterm infants who were born during the third trimester had poorer orbito-prefrontal development together with a significant reduction in the depth of the secondary orbital sulci (Gimenez *et al.*, 2006). The resultant overall cerebral volume with a higher growth rate after 28 weeks in the present study is consistent with a previous *in vitro* result (Chi *et al.*, 1977); furthermore, we have shown that the greater growth in cerebral volume is mainly contributed by the frontal lobe compared with other regions (Table 2).

In summary, we have investigated the regional differences between the growths in cerebral volume and in cortical convolutions for fetal brains. The plausible parcellations proposed in this study allow the regional analysis of brains *in utero*, without the risk of using sedation during fetal MRI scanning. The growth rates in gyrification across distinct brain areas exhibit no regional difference, suggesting that changes in size of cortical sheet in these regions may synchronize over time, which is in line with the hypothesis of tension from cortico-

cortical connection. On the other hand, we find that the increase in cerebral volume in the frontal and parieto-temporal regions can be confounded by the expansion of basal ganglia underlying these regions. This reveals that the cerebral volume is an unhelpful parameter to measure in relation to gyrification, and that changes in size of cortical sheet are more likely correlated with cortical folding.

Acknowledgements

This study was funded in part by the National Science Council (NSC-94-2314-B-075-056, NSC-95-2314-B-075-007, NSC-96-2314-B-075-005, NSC-97-2752-B-075-010-001-PAE) and Taipei Veterans General Hospital (V95C1-105, V96Cl-135, V97C1-025 and V97ER1-005). The authors appreciate reviewers' insightful comments and suggestions.

Abbreviations

CI, curvature index; F, frontal cortex; GI, gyrification index; GUI, graphical user interface; MRI, magnetic resonance imaging; O, occipital cortex; P&T, parieto-temporal cortex; PreF, prefrontal cortex; SNR, signal-to-noise ratio.

References

Armstrong, E., Curtis, M., Buxhoeveden, D.P., Fregoe, C., Zilles, K., Casanova, M.F. & McCarthy, W.F. (1991) Cortical gyrification in the Rhesus monkey: a test of the mechanical folding hypothesis. *Cereb. Cortex*, **1**, 426–432.

Armstrong, E., Schleicher, A., Omran, H., Curtis, M. & Zilles, K. (1995) The ontogeny of human gyrification. *Cereb. Cortex*, **5**, 56–63.

Aylward, E.H., Minshew, N.J., Field, K., Sparks, B.F. & Singh, N. (2002) Effects of age on brain volume and head circumference in autism. *Neurology*, **59**, 175–183.

Batchelor, P.G., Castellano Smith, A.D., Hill, D.L., Hawkes, D.J., Cox, T.C. & Dean, A.F. (2002) Measures of folding applied to the development of the human fetal brain. *IEEE Trans Med Imaging*, **21**, 953–965.

Bonnici, H.M., William, T., Moorhead, J., Stanfield, A.C., Harris, J.M., Owens, D.G., Johnstone, E.C. & Lawrie, S.M. (2007) Pre-frontal lobe gyrification index in schizophrenia, mental retardation and comorbid groups: an automated study. *Neuroimage*, **35**, 648–654.

Bradley, W.G., Daroff, R.B., Fenichel, G.M. & Marsden, C.D. (1991) *Neurology in Clinical Practice*. Butterworths, Boston.

Canny, J. (1986) A computational approach to edge detection. *IEEE Trans. Pattern Anal. Mach. Intell.*, **8**, 679–698.

Caviness, V.S. Jr (1975) Mechanical model of brain convolutional development. *Science*, **189**, 18–21.

Chi, J.G., Dooling, E.C. & Gilles, F.H. (1977) Gyral development of the human brain. *Ann. Neurol.*, **1**, 86–93.

Encha-Razavi, F. & Sonigo, P. (2003) Features of the developing brain. *Child's Nerv. Syst.*, **19**, 426–428.

Gilmore, J.H., Lin, W., Prastawa, M.W., Looney, C.B., Vetsa, Y.S.K., Knickmeyer, R.C., Evans, D.D., Smith, J.K., Hamer, R.M. & Lieberman, J.A. (2007) Regional gray matter growth, sexual dimorphism, and cerebral asymmetry in the neonatal brain. *J. Neurosci.*, **27**, 1255.

Gimenez, M., Junque, C., Vendrell, P., Narberhaus, A., Bargallo, N., Botet, F. & Mercader, J.M. (2006) Abnormal orbitofrontal development due to prematurity. *Neurology*, **67**, 1818.

Gonzales, R.C. & Woods, R.E. (2001) *Digital Image Processing*. Prentice Hall, New Jersey.

Grossman, R., Hoffman, C., Mardor, Y. & Biegon, A. (2006) Quantitative MRI measurements of human fetal brain development in utero. *Neuroimage*, **33**, 463–470.

Guo, W.Y. & Wong, T.T. (2003) Screening of fetal CNS anomalies by MR imaging. *Child's Nerv. Syst.*, **19**, 410–414.

Harris, J.M., Moorhead, T.W.J., Miller, P., McIntosh, A.M., Bonnici, H.M., Owens, D.G.C., Johnstone, E.C. & Lawrie, S.M. (2007) Increased prefrontal gyrification in a large high-risk cohort characterizes those who develop schizophrenia and reflects abnormal prefrontal development. *Biol. Psychiatry*, **62**, 722–729.

Luders, E., Thompson, P.M., Narr, K.L., Toga, A.W., Jancke, L. & Gaser, C. (2006) A curvature-based approach to estimate local gyrification on the cortical surface. *Neuroimage*, **29**, 1224–1230.

Magnotta, V.A., Andreasen, N.C., Schultz, S.K., Harris, G., Cizadlo, T., Heckel, D., Nopoulos, P. & Flaum, M. (1999) Quantitative in vivo measurement of gyrification in the human brain: changes associated with aging. *Cereb. Cortex*, **9**, 151–160.

Nishida, M., Makris, N., Kennedy, D.N., Vangel, M., Fischl, B., Krishnamoorthy, K.S., Caviness, V.S. & Grant, P.E. (2006) Detailed semiautomated MRI based morphometry of the neonatal brain: preliminary results. *Neuroimage*, **32**, 1041–1049.

Peterson, B.S., Vohr, B., Staib, L.H, Cannistraci, C.J., Dolberg, A., Schneider, K.C., Katz, K.H., Westerveld, M., Sparrow, S., Anderson, A.W., Duncan, C.C., Makuch, R.W., Gore, J.C. & Ment, L.R. (2000) Regional Brain Volume Abnormalities and Long-term Cognitive Outcome in Retern Infants. *JAMA*, **284**, 1939–1947.

Stanfield, A.C., Moorhead, T.W.J., Harris, J.M., Owens, D.G.C., Lawrie, S.M. & Johnstone, E.C. (2008) Increased right prefrontal cortical folding in adolescents at risk of schizophrenia for cognitive reasons. *Biol. Psychiatry*, **63**, 80–85.

Thirion, J.P. & Gourdon, A. (1993) *The Marching Lines Algorithm: New Results and Proofs*. INRIA Internal Report 1881, INRIA France Project Epidaure.

Thompson, P.M., Schwartz, C., Lin, R.T., Khan, A.A. & Toga, A.W. (1996) Three-dimensional statistical analysis of sulcal variability in the human brain. *J. Neurosci.*, **16**, 4261–4274.

Van Essen, D.C. (1997) A tension-based theory of morphogenesis and compact wiring in the central nervous system. *Nature*, **385**, 313–318.

White, T., Andreasen, N.C., Nopoulos, P. & Magnotta, V. (2003) Gyrification abnormalities in childhood- and adolescent-onset schizophrenia. *Biol. Psychiatry*, **54**, 418–426.

Zilles, K., Armstrong, E., Schleicher, A. & Kretschmann, H.J. (1988) The human pattern of gyrification in the cerebral cortex. *Anat. Embryol.*, **179**, 173–179.